Research Article

Shuguang Li, Yijie Li, Mohammed K. Al Mesfer, Kashif Ali, Wasim Jamshed*, Mohd Danish, Kashif Irshad, Sohail Ahmad, and Ahmed M. Hassan

Insights into the thermal characteristics and dynamics of stagnant blood conveying titanium oxide, alumina, and silver nanoparticles subject to Lorentz force and internal heating over a curved surface

https://doi.org/10.1515/ntrev-2023-0145
received June 22, 2023; accepted October 3, 2023

Abstract: It is very significant and practical to explore a triple hybrid nanofluid flow across the stuck zone of a stretching/shrinking curved surface with impacts from stuck and Lorentz force factors. The combination (Ag–TiO_2–Al_2O_3/blood) hybrid nanofluid is studied herein as it moves across a stagnation zone of a stretching/shrinking surface that curves under the impact of pressure and Lorentz force. Exact unsolvable nonlinear partial differential equations can be transformed into ordinary differential equations that can be solved numerically by similarity transformation. It was discovered that predominant heat transfers and movement characteristics of quaternary hybrid nanofluids are dramatically affected. Numerous data were collected from this study to illustrate how parameters of flow affect the temperature, velocity, heat transmission, and skin friction characteristics. The axial and radial velocities for both fluids (Newtonian and ternary hybrid nanofluid) are increased due to the increasing function of the curvature parameter, magnetic field, and suction parameter. Additionally, the direct relationship between the temperature and heat transfer decreases the heat transfer rate by the curvature parameter, magnetic field, suction parameter, Prandtl number, and heat source/sink. The higher the values of the curvature parameter, the higher the shear stress and velocity.

Keywords: ternary-hybrid nanoparticles, curved surface, MHD, heat source/sink, quasi-linearization method

Nomenclature

p	pressure field (ML/T^2)
k	dimensionless curvature parameter
ρ_{mnf}	nanofluid density (M/LT)
Pr	dimensionless Prandtl number
υ_{mnf}	fluid kinematic viscosity (L^2/T)
ϕ_2	concentration of titanium (mol/m^3)
α_{mnf}	nanofluid thermal diffusivity (L^2/T)
C_f	skin friction
σ_{mnf}	electrical conductivity (T^3A^2/ML^3)
μ_{mnf}	nanofluid dynamic viscosity (M/L^3)
ϕ_1	concentration of silver (mol/m^3)
M	dimensionless magnetic parameter
k_{mnf}	nanoparticles thermal conductivity (ML/T^3K)
ε	dimensionless suction parameter
$(\rho C_p)_{mnf}$	heat capacity (ML^2/T^2K)
ϕ_3	concentration of aluminum (mol/m^3)
Nu_s	Nusselt number

* **Corresponding author: Wasim Jamshed,** Department of Mathematics, Capital University of Science and Technology (CUST), Islamabad, 44000, Pakistan, e-mail: wasiktk@hotmail.com
Shuguang Li: School of Computer Science and Technology, Shandong Technology and Business University, Yantai 264005, China
Yijie Li: School of Computer Science, University of St Andrews, St Andrews KY16 9SX, United Kingdom
Mohammed K. Al Mesfer, Mohd Danish: Chemical Engineering Department, College of Engineering, King Khalid University, Abha, Saudi Arabia
Kashif Ali: Department of Basic Science and Humanities, Muhammad Nawaz Sharif University of Engineering and Technology, Multan 60000, Pakistan
Kashif Irshad: Interdisciplinary Research Centre for Renewable Energy and Power System (IRC-REPS), Research Institute, King Fahd University of Petroleum and Minerals (KFUPM), Dhahran, 31261, Saudi Arabia
Sohail Ahmad: Centre for Advanced Studies in Pure & Applied Mathematics, Bahauddin Zakariya University, Multan 60800, Pakistan
Ahmed M. Hassan: Center of Research, Faculty of Engineering, Future University in Egypt New Cairo 11835, Egypt

1 Introduction

Ag is often used to represent silver, which is a chemical element. It is considered to possess high reflectivity and is a metal with a lustrous white color. It contains special thermal characteristics and has various industrial uses. The flows involving silver nanoparticles have been interpreted by many researchers. Waqas *et al.* [1] studied the stenotic artery flow incorporating silver and gold nanoparticles. The pertinence of usage of the silver–gold combination was described, which was based on the potential drug transport phenomenon. The flow phenomenon was studied under a magnetic field effect. The enhancement in heat transfer through a water-based nanofluid containing Ag–H_2O was observed by Suleman *et al.* [2]. The results of this study were mainly based on a numerical analysis that was performed using a classical shooting method. Zhang *et al.* [3] explored numerical Ag–MgO/water hybrid nanofluid flow *via* a rotating disc, and the magnesium oxide and silver particles, owing to their special thermal features, were taken into account. They noticed an increasing effect on the velocity and heat energy transfer due to the spinning disc. Mousavi *et al.* [4] used the bvp4c built-in function in MATLAB to simulate the zinc oxide–silver/water flow neglecting the velocity slip effect. Their observation showed that skin friction and velocity would enhance when the disc rotated faster. A spinning flow of the hybrid nanofluid, which was prepared by mixing gold and silver particles in a liquid solution of ethylene glycol was premeditated by Alqahtani *et al.* [5]. In this work, the energy transport mechanism is discussed, specifically, using the Ag–Au nanoparticles.

Aluminum and oxygen when combined yield aluminum oxide, which is a chemical compound in nature. Aluminum oxide can be naturally found in different minerals but it can also be prepared synthetically. Ahmad *et al.* [6–8] investigated the water-based hybrid nature flow of nanofluids comprising aluminum oxide (Al_2O_3) and copper (Cu) nanoparticles. In their work, they examined a significant enhancement in the heat transfer in the case of hybrid nanocomposition of Al_2O_3–Cu/H_2O rather than the usual nanofluid case. An experimental study was performed by Murtadha and Hussein [9] to examine solar panel cooling incorporating the aluminum oxide nanofluid. Different flow rates at different concentrations of nanoparticles were used to elaborate the experimental results. Rahman *et al.* [10] carried out a study and discussed the heat transfer increase due to the correlation of the Cu–Al_2O_3 hybrid nanofluid considering water as a base fluid. Hassan *et al.* [11] reported the thermal performance of polyvinyl alcohol solutions when they interacted with aluminum oxide. The physical aspects of the parameters were numerically analyzed.

Titanium oxide (TiO_2) usually occurs naturally and is used widely in white pigment. It has various commercial applications. A mathematical approach toward finding the solution of nanofluid flow involving titanium oxide was performed by Arulprakasajothi *et al.* [12]. The friction factor was reduced but the Nusselt number increased by the nanoparticle fraction of TiO_2. An electromagnetohydrodynamics flow was considered by Ramesh *et al.* [13] where they studied the thermal performance of iron oxide and titanium oxide. The Eckert number was considered in the energy equation. However, a numerical technique was used in the dimensionless form of the governing equations which was obtained after similarity transformation. The oxide forms of titanium and aluminum were amalgamated in the blood by Khan *et al.* [14] to prepare the hybrid mixture of blood-based nanofluids. A vertical oscillating plate showed the flow mechanism. The mixed convection phenomenon was also considered, and simulations were done by the Caputo fractional simulation technique. Ahmad *et al.* [15] interpreted the role of titanium oxide (TiO_2) in the augmentation of the heat transmission rate. A linear stretched surface was considered as the geometry of the problem. It was assumed that the hybrid mixture would increase thermal efficiency more rigorously as compared to the mono nanofluids. An algorithmic approach based on the fifth-order Runge–Kutta method was employed by Hafeez *et al.* [16] to compute the solutions of the ternary nanofluid flow consisting of TiO_2, CuO, and Al_2O_3.

Blood flows have potential use in biosciences. Recently, many studies have been reported on the blood-based nanofluid flows due to their prominent applications. Sharma *et al.* [17] incorporated the response surface methodology to develop the model describing the blood-based nanofluid flow under the prominent viscosity and Hall effects. How the physical parameters altered the Nusselt number and skin friction were examined. A peristaltic blood flow was considered by Noreen *et al.* [18]. Blood is considered to be flowing within a vertical channel (an artery). The axial velocity and the pressure gradient were computed by numerical solutions. Elelamy *et al.* [19] provided a mathematical approach to finding the theoretical aspects of the Casson micropolar blood flow which was non-Newtonian. The magnetic permeability caused variations in the temperature of the fluid. Abeer *et al.* [20] and Saeed *et al.* [21] used the homotopy analysis method for the exploration of blood-based tri-hybrid (CuO–TiO_2–Al_2O_3) and hybrid (SWCNT and MWCNT) flows, respectively. Makinde and Animasaun [22,23] investigated the magnetohydrodynamic flows past an upper surface of a paraboloid with allowance for a chemical reaction.

Ternary nanofluids refer to a type of nanofluid that contains three different types of nanoparticles suspended

in a liquid. Nanofluids are engineered fluids that are created by suspending nanoparticles in a base fluid, such as water or oil. The addition of nanoparticles to the base fluid can significantly enhance its thermal, electrical, and mechanical properties, and Li *et al.* presented an analysis of using it [24]. Ternary nanofluids are of particular interest in research and development because they can offer even greater improvements in these properties compared to binary nanofluids, which contain only two types of nanoparticles [25,26]. By carefully selecting the types and concentrations of nanoparticles in a ternary nanofluid, it is possible to form a fluid with tailored properties that are optimized for a specific application. However, creating ternary nanofluids can be challenging, as the addition of a third nanoparticle type can lead to more complex interactions and behavior between the nanoparticles and the base fluid (see the study of Al Oweidi [27]). As a result, researchers must carefully study the thermodynamic, rheological, and transport properties of ternary nanofluids to fully understand their behavior and potential applications (see the study of Shahzad *et al.* [28]). Ternary nanofluids can be used as a catalyst in various chemical reactions, such as Fischer–Tropsch synthesis, where they can improve the conversion rate and selectivity of the reaction [29]. For further relevant work, see previous studies [30–35].

The purpose of this work is to investigate the novel flow and thermal characteristics of tri-hybrid nanofluids that are mainly based on silver, titanium dioxide, and aluminum dioxide. The proposed nano-composition (Ag–TiO_2–Al_2O_3/blood) has not been interpreted before being subjected to suction and Lorentz force. The analysis comprehends the features of ternary hybrid nanofluid and it also portrays the thermal characteristics of the Newtonian case of the nanofluid. The main effects of all physical parameters of the problem on the velocity, temperature, concentration, and surface drag are discussed in detail.

2 Mathematical formulation

This work examines a triple hybrid nanofluid formed by suspending Ag, TiO_2, and Al_2O_3 in blood as the base liquid in a predictable two-dimensional, inflexible MHD stagnant point movement. Figure 1 shows how a flow designer functions. In this case, mass sucking is equivalent to vw, so the radius R defines the permeable arched stretching/shrinking surface, and the temperature source/sink can be found by the curvy directs (r, s), where r is the normal to tangent vector at every point on the surface and s is the arc length coordinate alongside the path of movement route. The

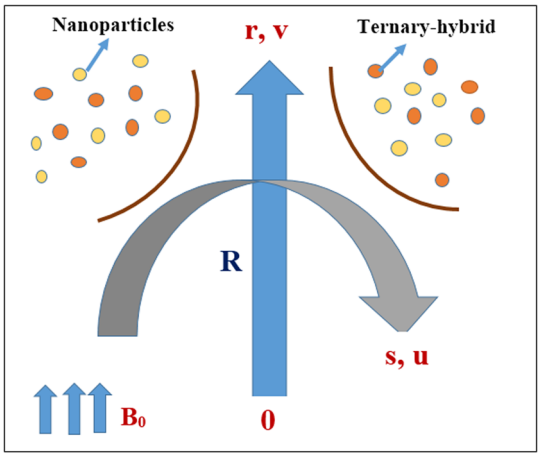

Figure 1: The flow configuration model of a curved surface.

configuration ensures that a modest distortion corresponds to a significant amount of the circumference R. It is additionally presumed that the mass transfer speed is vw, and when $vw > 0$, it denotes sucking and B_0 is the strength of the magnetic field.

Pressure does not continue as a constant during a border sheet, as given by Waini *et al.* [36]. Subsequently, it is incredible in the direction of the pressure gradient arranged by a curved surface. Now, it is theoretical that $u_e(s) = as$ with $a > 0$ and $T(s) = T_\infty + T_0(s/L)$, where T_∞ is the constant ambient heat, T_0 characterizes the source heat, and L is distance. It is conceivable to simplify the equations and reduce their similarity by choosing a heat that has already been settled upon for the surface. Numerous conceptual considerations are put forward in studying ternary nanofluids. The ternary nanofluid is anticipated to be stable. The base fluid and the nanoparticles are thought to be in thermal balance, meaning they are traveling at a comparable pace. Consequently, the effects of nanoparticle aggregating and settling are not considered. The nanoparticles are assumed to be of the same size and cylindrical in shape. In ternary hybrid nanofluids, these presumptions and boundary layer approximations result in controlling equations [36,37].

2.1 Model equations

$$\frac{\partial}{\partial r}((R + r)v) + R\frac{\partial u}{\partial s} = 0, \tag{1}$$

$$\frac{u^2}{R + r} = \frac{1}{\rho_{\text{mnf}}}\frac{\partial p}{\partial r}, \tag{2}$$

$$v\frac{\partial u}{\partial r} + \frac{Ru}{R+r}\frac{\partial u}{\partial s} + \frac{uv}{R+r} = -\frac{1}{\rho_{\mathrm{mnf}}}\frac{R}{R+r}\frac{\partial p}{\partial s} + \frac{\mu_{\mathrm{mnf}}}{\rho_{\mathrm{mnf}}}\left(\frac{\partial^2 u}{\partial r^2} + \frac{1}{R+r}\frac{\partial u}{\partial r} - \frac{u}{(R+r)^2}\right) - \frac{\sigma_{\mathrm{mnf}}}{\rho_{\mathrm{mnf}}}B_0^2(u-u_e), \tag{3}$$

$$v\frac{\partial T}{\partial r} + \frac{Ru}{R+r}\frac{\partial T}{\partial s} = \frac{k_{\mathrm{mnf}}}{(\rho C_{\mathrm{p}})_{\mathrm{mnf}}}\left(\frac{\partial^2 T}{\partial r^2} + \frac{1}{R+r}\frac{\partial T}{\partial r}\right) + \frac{Q}{(\rho C_{\mathrm{p}})_{\mathrm{mnf}}}(T - T_\infty). \tag{4}$$

Here, u and v characterize the speed module in s and r directions, respectively. The following are the principles that describe the limitations:

$$\left.\begin{aligned} u = u_{\mathrm{w}} = bs, v = v_{\mathrm{w}} = -\sqrt{av_f}\,\varepsilon, T = T_{\mathrm{w}}(s) \ \text{ at } \ r = 0, \\ u \to u_{\mathrm{e}}(s), \quad \frac{\partial u}{\partial r} \to 0, T \to T_\infty \ \text{ as } \ r \to \infty, \end{aligned}\right\} \tag{5}$$

where p is the pressure, $(\rho C_{\mathrm{p}})_{\mathrm{mnf}}$ represents the heat capacity of the nanofluid, u_{mnf} denotes the self-motivated viscidness, k_{mnf} embodies the current conductivity, ρ_{mnf} represents the thickness, Q represents the temperature source/sink measurement, and T represents the heat of the ternary hybrid nanofluid. According to Waini *et al.* [36], the situation should be shadowed; the succeeding correspondence alteration is currently presented as a means of incoming relationship solutions:

$$\begin{aligned} u = asf'(\eta), v = -\frac{R}{R+r}\sqrt{av_{\mathrm{f}}}\,f(\eta), p = \rho_f a^2 s^2 P(\eta), \\ \theta(\eta) = \frac{T - T_\infty}{T_{\mathrm{w}} - T_\infty}, \eta = \sqrt{\frac{a}{v_{\mathrm{f}})}}\,r. \end{aligned} \tag{6}$$

When distinguished with position to η, the prime shows the origin. One can obtain the ordinary differential equations that are prearranged below if we include (1), (2), (3), and (6) in the equations that describe the stable state. These are the equations that are displayed inferior to

$$p' = \rho_{\mathrm{mnf}}\frac{1}{K+\eta}f'^2, \tag{7}$$

$$\rho_{\mathrm{mnf}}\frac{2K}{K+\eta}p = \frac{\mu_{\mathrm{mnf}}}{\rho_{\mathrm{mnf}}}\left(f''' + \frac{1}{K+\eta}f'' - \frac{1}{(K+\eta)^2}f'\right) + \frac{K}{(K+\eta)^2}ff' - \frac{K}{K+\eta}f'^2 - M^2\frac{\sigma_{\mathrm{mnf}}}{\rho_{\mathrm{mnf}}}f'. \tag{8}$$

The following results are obtained by removing the pressure term P from these equations:

$$\frac{\mu_{\mathrm{mnf}}}{\rho_{\mathrm{mnf}}} + \left(f^{iv}\frac{2}{K+\eta}f''' - \frac{1}{(K+\eta)^2}f'' + \frac{1}{(K+\eta)^3}f'\right) + \frac{K}{K+\eta}(ff'' - f'f'') + \frac{K}{(K+\eta)^2}(ff'' - f'^2) - \frac{K}{(K+\eta)^3}ff' - M^2\frac{\sigma_{\mathrm{mnf}}}{\rho_{\mathrm{mnf}}}f'' - M^2\frac{1}{(K+\eta)}\frac{\sigma_{\mathrm{mnf}}}{\rho_{\mathrm{mnf}}}(f' - 1) = 0, \tag{9}$$

$$\frac{1}{P_{\mathrm{r}}}\frac{k_{\mathrm{mnf}}}{(\rho C_{\mathrm{p}})_{\mathrm{mnf}}}\left(\theta'' - \frac{1}{K+\eta}\theta'\right) + \frac{K}{K+\eta}(f\theta' - f'\theta) - \Omega\theta = 0. \tag{10}$$

Alteration of boundary situations (5) fixed by

$$\left.\begin{aligned} f(0) = \varepsilon, f'(0) = \delta, \theta(0) = 1, \\ f'(\eta) \to 1, f''(\eta) \to 0, \theta(\eta) \to 0, \ \text{ as } \ \eta \to \infty \end{aligned}\right\}. \tag{11}$$

The skin friction and Nusselt number are defined as

$$C_{\mathrm{f}} = \frac{1}{\rho_{\mathrm{f}}{u_{\mathrm{e}}}^2}\mu_{\mathrm{mnf}}\left(\frac{\partial u}{\partial r} - \frac{u}{R+r}\right)_{r=0}\theta'(0), \tag{12}$$

$$\mathrm{Nu}_s = -\frac{s}{k_{\mathrm{f}}(T_{\mathrm{w}} - T_\infty)}k_{\mathrm{mnf}}\left(\frac{\partial T}{\partial r}\right)_{r=0}. \tag{13}$$

Equations (6), (12) and (13) give

$$\mathrm{Re}_s^{\frac{1}{2}}C_{\mathrm{f}} = \frac{\mu_{\mathrm{mnf}}}{\mu_{\mathrm{f}}}f''(0), \tag{14}$$

$$\mathrm{Re}_s^{-\frac{1}{2}}\mathrm{Nu}_s = -\frac{k_{\mathrm{mnf}}}{k_{\mathrm{f}}}\theta'(0). \tag{15}$$

The thermal physical, nanofluids, hybrid nanofuids, ternary hybrid nanofluids properties, are given in Tables 1–4, respectively.

3 Numerical approach: quasi-linearization method (QLM)

QLM is a generalized form of the Newton–Raphson method which basically provides an algebraic sequence of functions. It transforms the nonlinear equations into linear ones from which the numerical solutions are obtained. The usual numerical techniques may not provide the solutions of equations (9) and (10) due to the involvement of coupled and non-linear terms. A constant of integration will also appear upon integrating the differential equations. There

Table 1: Mathematical standards of nanoparticles collected from ternary hybrids and blood [36]

Thermal physical traits	ρ (kg/m^3))	C_p (J/kgK)	k (W/mK)	σ (S/m)
Silver (ϕ_1)	10.5	235	429	3.6×10^7
Alumina (ϕ_2)	3,970	765	40	1.0×10^{-10}
Titanium oxide (ϕ_3)	4,250	686.2	8.9538	1.0×10^{-12}
Blood	1,063	0.492	3,594	0.8

Table 2: Principal assets of nanofluids

Properties	Nanofluids
Dynamics viscosity	$\mu_{nf} = \mu_f(1-\phi)^{-2.5}$
Consistency	$\rho_{nf} = (1-\phi)\rho_f + \phi\rho_s$
Heat capacity	$(\rho C_p)_{nf} = (1-\phi)(\rho C_p)_f + \phi(\rho C_p)_s$
Thermal conductance	$\frac{k_{nf}}{k_f} = \left[\frac{(k_s+2k_f)-2\phi(k_f-k_s)}{(k_s+2k_f)+\phi(k_f-k_s)}\right]$
Electrical conductivity	$\frac{\sigma_{nf}}{\sigma_f} = \left[1+\frac{3(\frac{\sigma_s}{\sigma_f}-1)\phi}{(\frac{\sigma_s}{\sigma_f}+2)-(\frac{\sigma_s}{\sigma_f}-1)\phi}\right]$

is no such mechanism that could directly find the value of this integration constant, and the only possibility is to find its value by hit and trial rule which may require a lot of time. The linearization of the system (9) and (10) will not face such type of inadequacy. However, quasi-linearization is the best approach for determining the approximate solutions of the problem. A detailed procedure of this technique is elaborated in our earlier work [38]. This technique is mainly based on the steps given in Figure 2a. Figure 2b

Table 3: Principal assets of hybrid nanofluids

Features	Hybrid nanofluid
Viscosity (u)	$\mu_{hnf} = \mu_f(1-\phi_1)^{-2.5}(1-\phi_2)^{-2.5}$
Density (ρ)	$\rho_{hnf} = [(1-\phi_2)\{(1-\phi_1)\rho_f + \phi_1\rho_{s_1}\}]+\phi_2\rho_{s_2}$
Heat capacity (ρC_p)	$(\rho C_p)_{hnf} = [(1-\phi_2)\{(1-\phi_1)(\rho C_p)_f + \phi_1(\rho C_p)_{p_1}\}] + \phi_2(\rho C_p)_{p_2}$
Thermal conductivity (κ)	$\frac{\kappa_{hnf}}{\kappa_{nf}} = \left[\frac{(\kappa_{s_2}+2\kappa_{nf})-2\phi_2(\kappa_{nf}-\kappa_{s_2})}{(\kappa_{s_2}+2\kappa_{nf})+\phi_2(\kappa_{nf}-\kappa_{s_2})}\right]$, where $\frac{\kappa_{nf}}{\kappa_f} = \left[\frac{(\kappa_{s_1}+2\kappa_f)-2\phi_1(\kappa_f-\kappa_{s_1})}{(\kappa_{s_1}+2\kappa_f)+\phi_1(\kappa_f-\kappa_{s_1})}\right]$
Electrical conductivity (σ)	$\frac{\sigma_{hnf}}{\sigma_{nf}} = \left[\frac{(\sigma_{s_2}+2\sigma_{nf})-2\phi_2(\sigma_{nf}-\sigma_{s_2})}{(\sigma_{s_2}+2\sigma_{nf})+\phi_2(\sigma_{nf}-\sigma_{s_2})}\right]$, where $\frac{\sigma_{nf}}{\sigma_f} = \left[\frac{(\sigma_{s_1}+2\sigma_f)-2\phi_1(\sigma_f-\sigma_{s_1})}{(\sigma_{s_1}+2\sigma_f)+\phi_1(\sigma_f-\sigma_{s_1})}\right]$

Table 4: Current and powered features of the ternary hybrid nanofluid

Features	Ternary hybrid nanofluid
Viscosity (u)	$\mu_{mnf} = \mu_f(1-\phi_1)^{-2.5}(1-\phi_2)^{-2.5}(1-\phi_3)^{-2.5}$
Density (ρ)	$\rho_{mnf} = (1-\phi_3)\{(1-\phi_2)[(1-\phi_1)\rho_f + \phi_1\rho_{s_1}] + \phi_2\rho_{s_2}\} + \phi_3\rho_{s_3}$
Heat capacity (ρC_p)	$(\rho C_p)_{mnf} = (1-\phi_3)\{(1-\phi_2)[(1-\phi_1)(\rho C_p)_f + \phi_1(\rho C_p)_{s_3}] + \phi_2(\rho C_p)_{s_2}\} + \phi_3(\rho C_p)_{s_3}$
Thermal conductivity (κ)	$\frac{\kappa_{mnf}}{\kappa_{hnf}} = \left[\frac{(k_{s_3}+2k_{hnf})-2\phi_3(k_{hnf}-k_{s_3})}{(k_{s_3}+2k_{hnf})+\phi_3(k_{hnf}-k_{s_3})}\right]$, where $\frac{\kappa_{hnf}}{\kappa_f} = \left[\frac{(k_{s_2}+2k_{nf})-2\phi_2(k_{nf}-k_{s_2})}{(k_{s_2}+2k_{nf})+\phi_2(k_{nf}-k_{s_2})}\right]$, $\frac{\kappa_{nf}}{\kappa_f} = \left[\frac{(k_{s_1}+2k_f)-2\phi_1(k_f-k_{s_1})}{(k_{s_1}+2k_f)+\phi_1(k_f-k_{s_1})}\right]$.
Electrical conductivity (σ)	$\frac{\sigma_{mnf}}{\sigma_{hnf}} = \left[\frac{(\sigma_{s_3}+2\sigma_{hnf})-2\phi_3(\sigma_{hnf}-\sigma_{s_3})}{(\sigma_{s_3}+2\sigma_{hnf})+\phi_3(\sigma_{hnf}-\sigma_{s_3})}\right]$, where $\frac{\sigma_{hnf}}{\sigma_{nf}} = \left[\frac{(\sigma_{s_2}+2\sigma_{nf})-2\phi_2(\sigma_{nf}-\sigma_{s_2})}{(\sigma_{s_2}+2\sigma_{nf})+\phi_2(\sigma_{nf}-\sigma_{s_2})}\right]$, $\frac{\sigma_{nf}}{\sigma_f} = \left[\frac{(\sigma_{s_1}+2\sigma_f)-2\phi_1(\sigma_f-\sigma_{s_1})}{(\sigma_{s_1}+2\sigma_f)+\phi_1(\sigma_f-\sigma_{s_1})}\right]$.

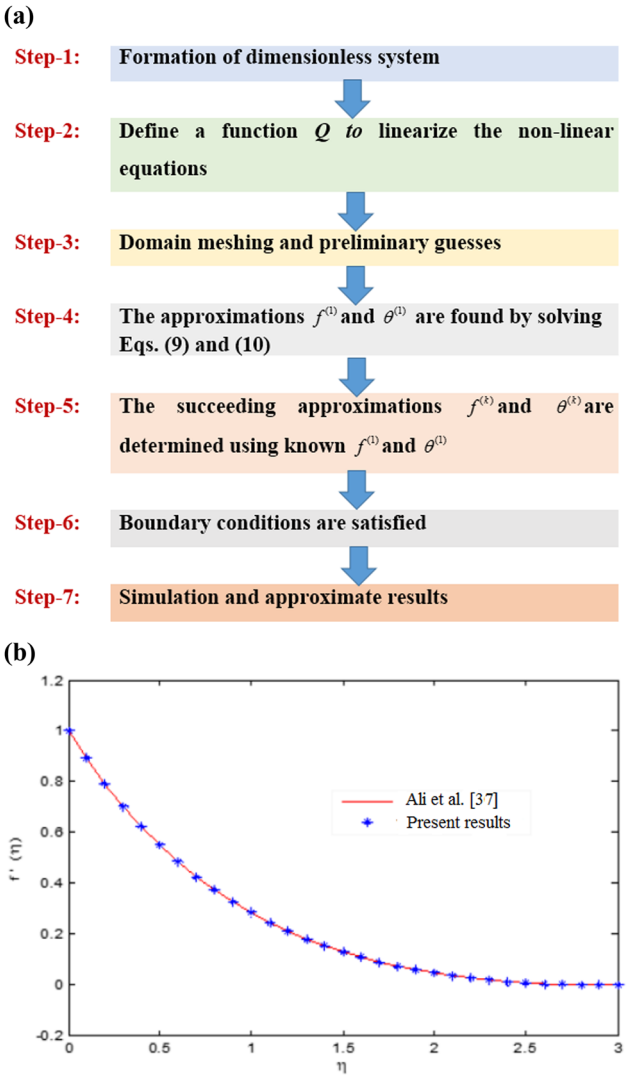

Figure 2: (a) A flow chart of QLM. (b) Comparison of the present numerical results with those of Ali *et al.* [39].

represents the comparison of the present numerical results with those presented by Ali *et al.* [39].

4 Results and discussions

The QLM is implemented to provide the numerical solutions of equations (9) and (10), together with the boundary requirement (11) and physical parameters (14), and (15) which have been described in the previous section. In this section, information and positions are utilized to demonstrate the numerical results.

Fixed values of the parameters are: $k = 5$, $M = 2$, $\varepsilon = 0.04$, Pr = 6.2, Rn = 0.5.

For Newtonian case: $\phi_1 = 0.00; \phi_2 = 0.00; \phi_3 = 0.00$.

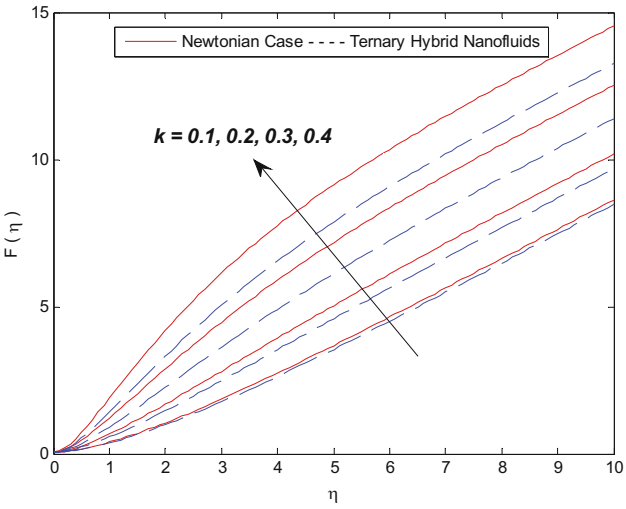

Figure 3: Variation in $F(\eta)$ for different values of k.

For ternary hybrid nanofluids: $\phi_1 = 0.03$; $\phi_2 = 0.06$; $\phi_3 = 0.1$.

The data are the profiles of axial velocity $F(\eta)$, radial velocity $F'(\eta)$, and temperature $\theta(\eta)$. These profiles contain the Newtonian and ternary (Ag–TiO_2–Al_2O_3/blood) hybrid nanofluid curves, which meet the far-field boundary requirements (11). All data present the greater velocity with the Newtonian fluid, whereas the higher fluid temperature with the ternary hybrid nanofluid. All the controlling parameters, such as $k = 0.1, 0.2, 0.3, 0.4$ (the curvature parameter), $M = 3, 5, 7, 9$ (the magnetic field parameter), Pr = 1, 3, 5, 7 (the Prandtl number), Rn = 0, 1, 2, 3 (the heat source/sink parameter), and Pr = 1, 3, 5, 7 (the suction parameter) are selected to produce these profiles as depicted in Figure 3 and S5.

4.1 Discussion

The profiles against the curvature parameter are shown in Figures 3–5 for the axial velocity, radial velocity, and temperature. In detail, Figure 1 shows the impact of k on the velocity. Figures 3 and 4 show that higher k indicates an inciting nature in the axial and radial velocities. Meanwhile, increasing k indicates a weak temperature distribution as displayed in Figure 5. Figures 6 and 7 show the magnetic field influence on the velocity in the axial and radial components, together with the temperature curves of the Newtonian and ternary hybrid nanofluid. The figures contradict the theory of the effect of the magnetic field on the velocity distribution, where the magnetic field containing the Lorentz force should act against the direction of the velocity itself. Figures 6 and 7 prove that the Lorentz force still plays a role by reducing the interaction between molecules. However, this force produces

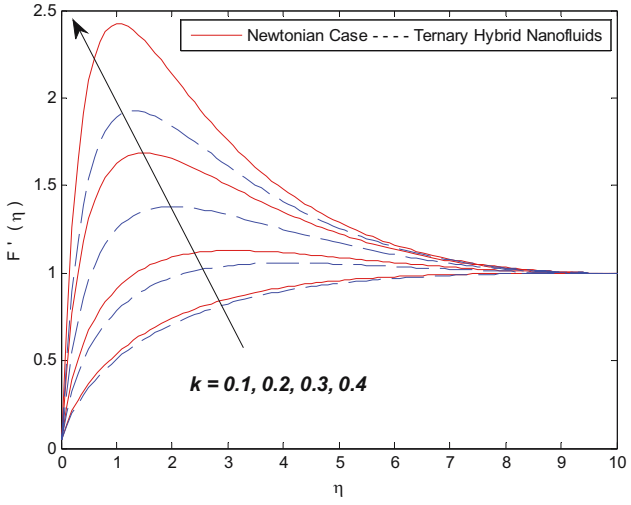

Figure 4: Variation in $F'(\eta)$ for different values of k.

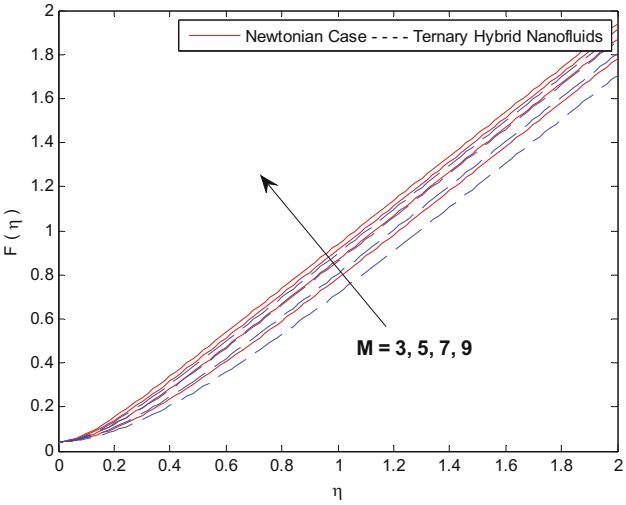

Figure 6: Variation in $F(\eta)$ for different values of M.

different results by increasing the velocity values. When the axial and radial velocities of the flow are increased, more thermal energy may be absorbed by fluid particles, and temperatures will become higher due to the effect of M (Figure 8). The temperature profile against the Prandtl number is shown in Figure S1, which indicates that the higher Pr suppresses the temperature profile because Pr increases the fluid viscosity. Consequently, the wall friction is augmented together with thermal conductivity. Therefore, finally, the temperature profile is decreased.

Figure S2 gives the variation of temperature distribution within the boundary layer for diverse values of heat source/sink parameters for Newtonian and ternary hybrid nanofluid cases. The increase in the velocities distribution in the axial (Figure S3) and radial components (Figure S4) can be observed in conjunction with increasing suction ε. The association between heat and ε is shown in Figure S5. These parameters remain constant unless they are declared in certain tables: $k = 5$, $M = 2$, $\varepsilon = 0.04$, Pr = 6.2, Rn = 0.5. Meanwhile, the fixed values for the Newtonian and ternary hybrid nanofluids are $\phi_1 = 0.00$; $\phi_2 = 0.00$; $\phi_3 = 0.00$ and $\phi_1 = 0.03$; $\phi_2 = 0.06$; $\phi_3 = 0.1$, respectively. The influence of k and M on $f''(0)$ and $\theta'(0)$ are shown in Table 5. An additional conclusion that can be inferred from Table 2 is that when k increases, the shear stress also increases. This observation can be explained by the fact that the velocity gradient at the wall is higher for the curved surface compared to the curved surfaces which tend to be flattening at the same position. Table 5 shows that the convective heat transmission amount of a curved surface with a small curvature is more significant than the same

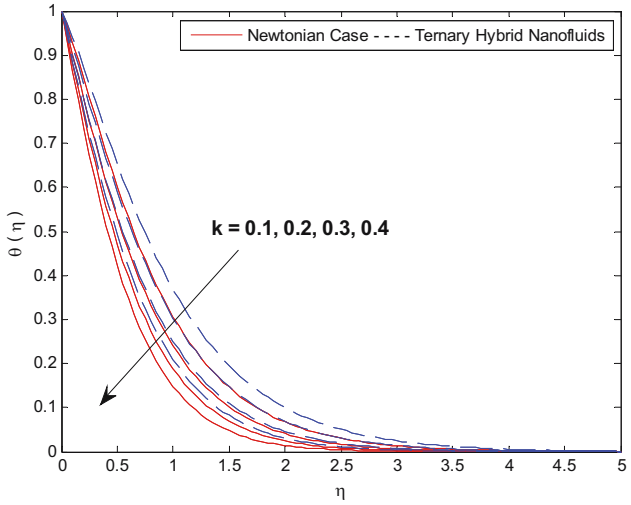

Figure 5: Variation in $\theta(\eta)$ for different values of k.

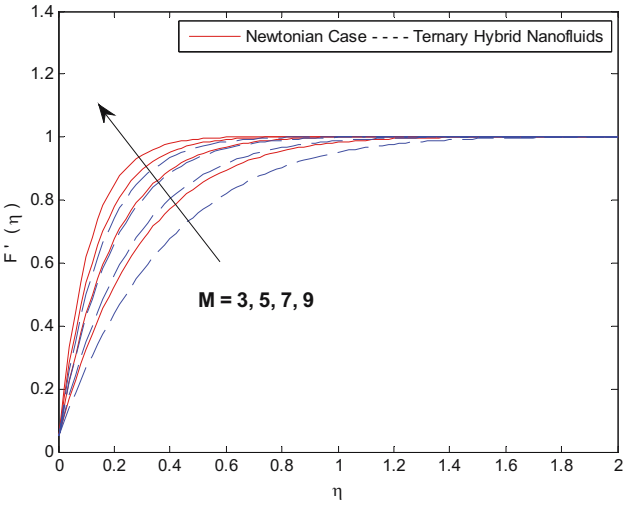

Figure 7: Variation in $F'(\eta)$ for different values of M.

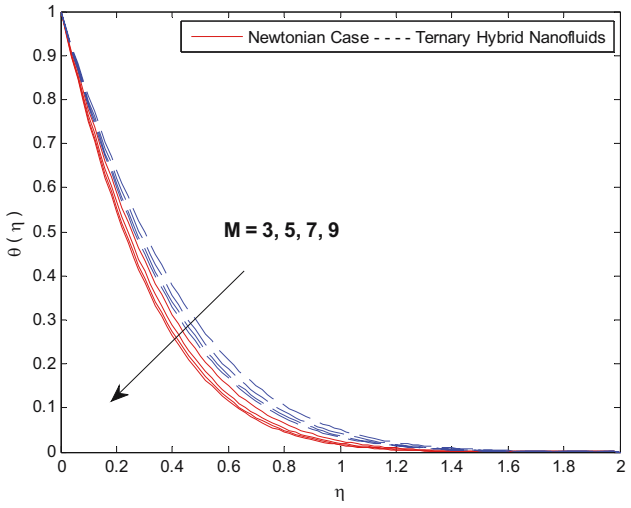

Figure 8: Variation in $\theta(\eta)$ for different values of M.

surface with a higher curvature. This proves that heat transfer reduces when k increases. Moreover, it can be noted from Table 5 that $f''(0)$ is an augmenting function of the magnetic field parameter and $\theta'(0)$ decreases with the same parameter. Table 6 lists the values of the shear stress and heat transfer for the suction parameter ε; the results indicate that Newtonian fluid has a lower heat transfer rate compared with the ternary hybrid nanofluid. The behavior of the heat transfer acted by Pr and Rn is shown in Table 7. There is a decrease in the heat transfer subjected to the increasing heat source/sink. With a stronger heat source, a larger region of the thermal boundary layer decelerates the heat transfer rate.

4.2 Analysis of the results

From the results of parameters k and M, it is very clear that some of the shear stress values at the wall are negative, whereas others are positive. The negative shear stress indicates that the curved surface exerts a dragging force on the fluid, whereas the opposite nature is implied by the positive shear stress. Suction is compulsory to increase the shear stress, but it reduces the heat transfer of the Newtonian and ternary hybrid nanofluids at the same time. The results of this study also reveal that the ternary hybrid nanofluid has better thermal properties as compared to the Newtonian fluid since it contains three different types of nanoparticles: These nanoparticles have excellent thermal features (in the case of ternary hybrid nanofluids) to achieve efficient heat transfer. Besides, heat transfer is suppressed by Pr, where this parameter decreases the fluid temperature and subsequently the heat transfer. It is noted that the thermal boundary layer reduces with an increase in the heat source/sink parameter. As a result, the fluid temperature decreases with Rn.

Table 5: Change in the shear stress and heat transfer rate for various values of k and M

		$f''(0)$		$\theta'(0)$	
k	M	Newtonian case	Ternary case of hybrid nanofluids	Newtonian case	Ternary case of hybrid nanofluids
0.1		−1.203238616629410	−1.259578166385444	−0.555094490410257	−0.443910424529403
0.2		0.591823760046073	0.514802306034179	−1.030097125481055	−0.828961490026320
0.3		1.067970150592235	0.981804387289453	−1.394922781265906	−1.132797556986670
0.4		1.239132602295912	1.149268009599802	−1.668437712930249	−1.366794042494590
	3	1.686277239651979	1.261786968376755	−3.260276600035172	−2.809430460133622
	5	2.620266613722611	1.871398759283882	−3.352713655141870	−2.879428653940952
	7	3.586223889675000	2.525473608085416	−3.420647625707729	−2.936120577235041
	9	4.559797513595254	3.193281891289979	−3.471778128921688	−2.980952856077146

Table 6: Change in the shear stress and heat transfer rate for various values of ε

ε	$f''(0)$		$\theta'(0)$	
	Newtonian case	Ternary case of hybrid nanofluids	Newtonian case	Ternary case of hybrid nanofluids
1	1.058650792336024	0.973895167470928	−8.046345793990495	−6.488935867727203
3	1.828905137060133	1.622767436195716	−21.205294385699691	−16.704695557817573
5	2.723427076691820	2.389116363907817	−34.456276171561939	−27.176208353688637
7	3.662563539492680	3.199403894669217	−47.263019055568591	−37.446009795628839

Table 7: Change in the heat transfer rate for various values of Pr and Rn

Pr	Rn	$\theta'(0)$	
		Newtonian case	**Ternary case of hybrid nanofluids**
1		−1.172136251081740	−1.046581613409547
3		−2.004968974201304	−1.762915866537146
5		−2.613896722269793	−2.289312058933390
7		−3.129109076232328	−2.732516485490855
	0	−3.011935135301480	−2.629217711295500
	1	−4.043186641655977	−3.539006876378919
	2	−4.866417487532693	−4.266047375379184
	3	−5.568631606197178	−4.886564013028472

The results show that a higher k (curvature parameter) indicates an inciting nature in the axial and radial velocities. An increase in k reduces the curved surface's radius, causing a decreased interaction of fluid particles with this surface. The subsequent effect is that the resistance acting on the fluid flow decreases, and finally, the fluid axial and radial velocities are increased significantly. Meanwhile, the increase in k indicates a weak temperature distribution. It has also been observed that the Lorentz force still plays a role by reducing the interaction between molecules. However, this force produces different results by increasing the velocity values. When the flow axial and radial velocities are enhanced, more thermal energy may be absorbed by fluid particles, and temperatures will increase due to the effect of the magnetic field.

The presence of suction causes the additional particles to flow into the fluid system, which results in a density decrease. Suction also causes the complexity of the motion barricade layer to be decreased. Because of suction, the fluid flow is increased. Therefore, the supplementary energy is propagated into the momentum boundary layer as the Lorentz force increases against time. Meanwhile, the heat transfer of the surface with the lower curvature is greater than the surface with the greater curvature. Some parametric effects on the physics of several problems are given in previous studies [40–47].

5 Conclusions

This study considered the flow and thermal properties of a ternary nanofluid, where the base fluid is engine oil, and the nanoparticles submerged in the engine oil are copper, titanium dioxide, and silicon dioxide. The ternary hybrid nanofluid flows around a stagnation region of a stretching/shrinking curved surface, where this fluid system is subjected to additional factors such as magnetic field, suction, and heat source/sink. The appropriate similarity conversions and non-dimensional quantities were implemented to reduce the governing equations system and transform this system into a simplified version. A numerical calculation, such as QLM, was chosen to obtain the final solutions. The impact of diverse factors on the velocity in the axial and radial components, temperature, shear stress, and heat transfer are illustrated in figures and tables. Furthermore, a comparison thermal efficiency of the ternary hybrid nanofluid and conventional Newtonian fluid is also being discussed.

Fixed values of the parameters are:

$k = 5,\ M = 2,\ \varepsilon = 0.04,\ \mathrm{Pr} = 6.2,\ \mathrm{Rn} = 0.5$

For Newtonian case:

$\phi_1 = 0.00;\ \phi_2 = 0.00;\ \phi_3 = 0.00;$

For ternary hybrid nanofluids:

$\phi_1 = 0.03;\ \phi_2 = 0.06;\ \phi_3 = 0.1.$

From the findings as presented previously, the following results can be deduced:

1) The axial and radial velocities for both fluids (Newtonian and ternary hybrid nanofluids) are increased due to the increasing function of the curvature parameter, magnetic field, and suction parameter. These parameters increase the thickness of the momentum boundary layer and cause an increase in the axial and radial velocities.
2) The thermal boundary layer is suppressed by all the involved parameters such as the curvature parameter, magnetic field, suction parameter, Prandtl number, and heat source/sink. Therefore, there is always a decrease in the temperature for the ternary hybrid nanofluid and Newtonian fluid under these restricting parameters in this fluid flow model.
3) Since velocity and shear stress are related to each other, the increase of the velocity profile due to the related parameters also causes the shear stress to increase with the same governing parameters (curvature parameter, magnetic field, suction parameter).
4) The direct relationship between the temperature and heat transfer decreases the heat transfer by the curvature parameter, magnetic field, suction parameter, Prandtl number, and heat source/sink.

In the future, the present method might be used in several physical and technical problems [48–59].

Acknowledgments: The authors extend their appreciation to the Ministry of Education in KSA for funding this research work through the project number KKU-IFP2-H-4.

Funding information: The authors extend their appreciation to the Ministry of Education in KSA for funding this research work through the project number KKU-IFP2-H-4.

Author contributions: All authors have accepted responsibility for the entire content of this manuscript and approved its submission.

Conflict of interest: The authors state no conflict of interest.

References

[1] Waqas H, Farooq U, Liu D, Alghamdi M, Noreen S, Muhammad T. Numerical investigation of nanofluid flow with gold and silver nanoparticles injected inside a stenotic artery. Mater Des. 2022;223:111130. doi: 10.1016/j.matdes.2022.111130.

[2] Suleman M, Ramzan M, Ahmad S, Lu D, Muhammad T, Chung JD. A numerical simulation of silver–water nanofluid flow with impacts of Newtonian heating and homogeneous-heterogeneous reactions past a nonlinear stretched cylinder. Symmetry. 2019;11:295. doi: 10.3390/sym11020295.

[3] Zhang XH, Algehyne EA, Alshehri MG, Bilal M, Khan MA, Muhammad T. The parametric study of hybrid nanofluid flow with heat transition characteristics over a fluctuating spinning disk. PLoS One. 2021;16(8):e0254457. doi: 10.1371/journal.pone.0254457.

[4] Mousavi SM, Yousefi M, Rostami MN. Zinc oxide–silver/water hybrid nanofluid flow toward an off-centered rotating disk using temperature-dependent experimental-based thermal conductivity. Heat Transf. 2022;51:4169–86.

[5] Alqahtani AM, Bilal M, Ali A, Alsenani TR, Eldin SM. Numerical solution of an electrically conducting pinning flow of hybrid nanofluid comprised of silver and gold nanoparticles across two parallel surfaces. Sci Rep. 2023;13:7180. doi: 10.1038/s41598-023-33520-5.

[6] Ahmad S, Ali K, Rizwan M, Ashraf M. Heat and mass transfer attributes of Copper-Aluminum oxide hybrid nanoparticles flow through a porous medium. Case Stud Therm Eng. 2021;25:100932. doi: 10.1016/j.csite.2021.100932.

[7] Ahmad S, Ali K, Ashraf M. MHD flow of Cu-Al2O3/water hybrid nanofluid through a porous media. J Porous Media. 2021;24(7):61–73. doi: 10.1615/JPorMedia.2021036704.

[8] Ali K, Ahmad S, Nisar KS, Faridi AA, Ashraf M. Simulation analysisof MHD hybrid Cu-Al2O3/H2O nanofluid flowwith heat generation through a porous media. Int J Energy Res. 2021;45(13):19165–79. doi: 10.1002/er.7016.

[9] Murtadha TK, Hussein AA. Optimization the performance of photovoltaic panels using aluminum-oxide nanofluid as cooling fluid at different concentrations and one-pass flow system. Res Eng. 2022;15:100541.

[10] Rahman M, Ferdows M, Shamshuddin MD, Koulali A, Eid MR. Aiding (opponent) flow of hybrid copper–aluminum oxide nanofluid towards an exponentially extending (lessening) sheet with thermal radiation and heat source (sink) impact. J Pet Sci Eng Part B. 2022;215:110649. doi: 10.1016/j.petrol.2022.110649.

[11] Hassan M, Faisal A, Bhatti MM. Interaction of aluminum oxide nanoparticles with flow of polyvinyl alcohol solutions base nanofluids over a wedge. Appl Nanosci. 2018;8:53–60. doi: 10.1007/s13204-018-0651-x.

[12] Arulprakasajothi M, Elangovan K, Reddy KH, Suresh S. Heat transfer study of water-based nanofluids containing titanium oxide nanoparticles. Mater Today Proc. 2015;2:3648–55. doi: 10.1016/j.matpr.2015.07.123.

[13] Ramesh K, Asogwa KK, Oreyeni T, Reddy MG, Verma A. EMHD radiative titanium oxide-iron oxide/ethylene glycol hybrid nanofluid flow over an exponentially stretching sheet. Biomass Conv Bioref. 2023. doi: 10.1007/s13399-023-04033-y.

[14] Khan MI, Mansir IB, Raza A, Khan SU, Elattar S, Said HM, et al. Fractional simulations for thermal flow of hybrid nanofluid with aluminum oxide and titanium oxide nanoparticles with water and blood base fluids. Nanotechnol Rev. 2022;11(1):2757–67. doi: 10.1515/ntrev-2022-0156.

[15] Ahmad S, Ali K, Faridi AA, Ashraf M. Novel thermal aspects of hybrid nanoparticles Cu-TiO2 in the flow of ethylene glycol. Int Commun Heat Mass Transf. 2021;129:105708. doi: 10.1016/j.icheatmasstransfer.2021.105708.

[16] Bilal Hafeez M, Krawczuk M, Jamshed W, Tag El Din ES, El-Wahed Khalifa HA, Aziz ElSeabee FA. Thermal energy development in magnetohydrodynamic flow utilizing titanium dioxide, copper oxide and aluminum oxide nanoparticles: Thermal dispersion and heat generating formularization. Front Energy Res. 2022;10:1000796. doi: 10.3389/fenrg.2022.1000796.

[17] Sharma M, Sharma BK, Khanduri U, Mishra NK, Noeiaghdam S, Fernandez-Gamiz U. Optimization of heat transfer nanofluid blood flow through a stenosed artery in the presence of Hall effect and hematocrit dependent viscosity. Case Stud Therm Eng. 2023;47:103075. doi: 10.1016/j.csite.2023.103075.

[18] Noreen S, Rashidi MM, Qasim M. Blood flow analysis with considering nanofluid effects in vertical channel. Appl Nanosci. 2017;7:193–9. doi: 10.1007/s13204-017-0564-0.

[19] Elelamy AF, Elgazery NS, Ellahi R. Blood flow of MHD non-Newtonian nanofluid with heat transfer and slip effects: Application of bacterial growth in heart valve. Int J Numer Methods Heat Fluid Flow. 2020;30(No. 11):4883–908. doi: 10.1108/HFF-12-2019-0910.

[20] Alnahdi AS, Nasir S, Gul T. Blood-based ternary hybrid nanofluid flow-through perforated capillary for the applications of drug delivery. Waves Random Complex Media. 2022. doi: 10.1080/17455030.2022.2134607.

[21] Saeed A, Alsubie A, Kumam P, Nasir S, Gul T, Kumam W. Blood based hybrid nanofluid flow together with electromagnetic field and couple stresses. Sci Rep. 2021;11:12865. doi: 10.1038/s41598-021-92186-z.

[22] Makinde OD, Animasaun IL. Thermophoresis and Brownian motion effects on MHD bioconvection of nanofluid with nonlinear thermal radiation and quartic chemical reaction past an upper horizontal surface of a paraboloid of revolution. J Mol Liq. 2016;221:733–43.

[23] Makinde OD, Animasaun IL. Bioconvection in MHD nanofluid flow with nonlinear thermal radiation and quartic autocatalysis chemical reaction past an upper surface of a paraboloid of evolution. Int J Therm Sci. 2016;109:159–71.

[24] Li S, Puneeth V, Saeed AM, Singhal A, Al-Yarimi FA, Khan MI, et al. Analysis of the Thomson and Troian velocity slip for the flow of ternary nanofluid past a stretching sheet. Sci Rep. 2023;13:2340.

[25] Abdalla AN, Shahsavar A. An experimental comparative assessment of the energy and exergy efficacy of a ternary nanofluid-based photovoltaic/thermal system equipped with a sheet-and-serpentine tube collector. J Clean Prod. 2023;395:136460.

[26] Shahzad F, Jamshed W, El Din SM, Shamshuddin M, Ibrahim RW, Raizah Z, et al. Second-order convergence analysis for Hall effect and electromagnetic force on ternary nanofluid flowing via rotating disk. Sci Rep. 2022;12:18769.
[27] Al Oweidi KF, Shahzad F, Jamshed W, Usman, Ibrahim RW, El Din ESMT, et al. Partial differential equations of entropy analysis on ternary hybridity nanofluid flow model via rotating disk with hall current and electromagnetic radiative influences. Sci Rep. 2022;12:20692.
[28] Shahzad F, Jamshed W, Eid MR, Ibrahim RW, Aslam F, Siti SPMI, et al. The effect of pressure gradient on MHD flow of a tri-hybrid Newtonian nanofluid in a circular channel. J Magn Magn Mater. 2023;568:170320.
[29] Nguyen HM, Phan CM, Liu S, Pham-Huu C, Nguyen-Dinh L. Radio-frequency induction heating powered low-temperature catalytic CO2 conversion via bi-reforming of methane. Chem Eng J. 2022;430:132934.
[30] Cao W, Animasaun IL, Yook SJ, Oladipupo VA, Ji X. Simulation of the dynamics of colloidal mixture of water with various nanoparticles at different levels of partial slip: Ternary-hybrid nanofluid. Int Commun Heat Mass Transf. 2022;135:106069. doi: 10.1016/j.icheatmasstransfer.2022.106069.
[31] Saleem S, Animasaun IL, Yook SJ, Al-Mdallal QM, Shah NA, Faisal M. Insight into the motion of water conveying three kinds of nanoparticles shapes on a horizontal surface: Significance of thermomigration and Brownian motion. Surf Interfaces. 2022;30:101854. doi: 10.1016/j.surfin.2022.101854.
[32] Ali A, Das S, Jana RN. Oblique rotational dynamics of chemically reacting tri-hybridized nanofluids over a suddenly moved plate subject to Hall and ion slip currents, Newtonian heating and mass fluxes. J Indian Chem Soc. 2023;100(4):100983. doi: 10.1016/j.jics.2023.100983.
[33] Ali A, Das S, Jana RN. MHD gyrating stream of non-Newtonian modified hybrid nanofluid past a vertical plate with ramped motion, Newtonian heating and Hall currents. ZAMM. 2023;e202200080. doi: 10.1002/zamm.202200080.
[34] Amundson I, Kushwaha M, Koutsoukos X. A Method for Estimating Angular Separation in Mobile Wireless Sensor Networks. J Intell Robot Syst. 2013;71:273–86. doi: 10.1007/s10846-012-9788-0.
[35] Mercer E, Slind K, Amundson I, Cofer D, Babar J, Hardin D. Synthesizing verified components for cyber assured systems engineering. Softw Syst Model. 2023;22(5):1451–71. doi: 10.1007/s10270-023-01096-3.
[36] Waini I, Ishak A, Pop I. Flow towards a Stagnation Region of a Curved Surface in a Hybrid Nanofluid with Buoyancy Effects. Mathematics. 2021;9(18):2330.
[37] Zhang XH, Abidi A, Ahmed AE, Khan MR, El-Shorbagy MA, Shutaywi M, et al. MHD stagnation point flow of nanofluid over a curved stretching/shrinking surface subject to the influence of Joule heating and convective condition. Case Stud Therm Eng. 2021;26:101184.
[38] Ali K, Faridi AA, Ahmad S, Jamshed W, Khan N, Alam MM. Quasi-linearization analysis for heat and mass transfer of magnetically driven 3rd-grade (Cu-TiO2/engine oil) nanofluid via a convectively heated surface. Int Commun Heat Mass Transf. 2022;135:106060.
[39] Ali K, Jamshed W, Ahmad S, Bashir H, Ahmad S, Tag El Din ESM. A self-similar approach to study nanofluid flow driven by a stretching curved sheet. Symmetry. 2022;14:1991. doi: 10.3390/sym14101991.
[40] Elnaqeeb T, Animasaun IL, Shah NA. Ternary-hybrid nanofluids: significance of suction and dual-stretching on three-dimensional flow of water conveying nanoparticles with various shapes and densities. Z Naturforsch A. 2021;76(3):231–43.
[41] Animasaun IL, Yook SJ, Muhammad T, Mathew A. Dynamics of ternary-hybrid nanofluid subject to magnetic flux density and heat source or sink on a convectively heated surface. Surf Interfaces. 2022;28:101654.
[42] Asogwa KK, Mebarek-Oudina F, Animasaun IL. Comparative investigation of water-based Al2O3 nanoparticles through water-based CuO nanoparticles over an exponentially accelerated radiative riga surface. Arab J Sci Eng. 2022;47(7):8721–38.
[43] Sandeep N, Koriko OK, Animasaun IL. Modified kinematic viscosity model for 3D-Casson fluid flow within boundary layer formed on a surface at absolute zero. J Mol Liq. 2016;221:1197–206.
[44] Anantha Kumar K, Sandeep N, Sugunamma V, Animasaun IL. Effect of irregular heat source/sink on the radiative thin film flow of MHD hybrid ferrofluid. J Therm Anal Calorim. 2020;139:2145–53.
[45] Mahanthesh B, Gireesha BJ, Animasaun IL, Muhammad T, Shashikumar NS. MHD flow of SWCNT and MWCNT nanoliquids past a rotating stretchable disk with thermal and exponential space dependent heat source. Phys Scr. 2019;94:085214.
[46] Mahanthesh B, Lorenzini G, Oudina FM, Animasaun IL. Significance of exponential space-and thermal-dependent heat source effects on nanofluid flow due to radially elongated disk with Coriolis and Lorentz forces. J Therm Anal Calorim. 2020;141:37–44.
[47] Animasaun IL, Sandeep N. Buoyancy induced model for the flow of 36 nm alumina-water nanofluid along upper horizontal surface of a paraboloid of revolution with variable thermal conductivity and viscosity. Powder Technol. 2016;301:858–67.
[48] Koriko OK, Animasaun IL, Mahanthesh B, Saleem S, Sarojamma G, Sivaraj R. Heat transfer in the flow of blood-gold Carreau nanofluid induced by partial slip and buoyancy. Heat Transf - Asian Res. 2018;47(6):806–23. doi: 10.1002/htj.21342.
[49] Koriko OK, Adegbie KS, Shah NA, Animasaun IL, Olotu MA. Numerical solutions of the partial differential equations for investigating the significance of partial slip due to lateral velocity and viscous dissipation: The case of blood-gold Carreau nanofluid and dusty fluid. Numer Methods Partial Differ Equ. In-press. 2021;1–29. doi: 10.1002/num.22754.
[50] Vaidya H, Animasaun IL, Prasad KV, Rajashekhar C, Viharika JU, Al-Mdallal QM. , Nonlinear dynamics of blood passing through an overlapped stenotic artery with copper nanoparticles. J Non-Equilib Thermodyn. 2022;48(2):159–78. doi: 10.1515/jnet-2022-0063.
[51] Khan U, Zaib A, Ishak A, Abu Bakar S, Animasaun IL, Yook SJ. Insights into the dynamics of blood conveying gold nanoparticles on a curved surface when suction, thermal radiation, and Lorentz force are significant: The case of Non-Newtonian Williamson fluid. Math Comput Simul. 2021;193:250–68. doi: 10.1016/j.matcom.2021.10.014.
[52] Jamshed W, Aziz A. A comparative entropy based analysis of Cu and Fe_3O_4/methanol powell-eyring nanofluid in solar thermal collectors subjected to thermal radiation variable thermal conductivity and impact of different nanoparticles shape. Results Phys. 2018;9:195–205.
[53] Hussain SM, Jamshed W. A comparative entropy-based analysis of tangent hyperbolic hybrid nanofluid flow: Implementing finite difference method. Int Commun Heat Mass Transf. 2021;129:105671.
[54] Jamshed W, Devi SU, Nisar KS. Single phase-based study of Ag-Cu/EO Williamson hybrid nanofluid flow over a stretching surface with shape factor. Phys Scr. 2021;96:065202.

[55] Jamshed W, Gowda RJP, Kumar RN, Prasannakumara BC, Nisar KS, Mahmoud O, et al. Entropy production simulation of second-grade magnetic nanomaterials flowing across an expanding surface with viscidness dissipative flux. Nanotechnol Rev. 2022;11:2814–26.
[56] Shahzad F, Jamshed W, Safdar R, Mohd Nasir NAA, Eid MR, Alanazi MM, et al. Thermal valuation and entropy inspection of second-grade nanoscale fluid flow over a stretching surface by applying Koo–Kleinstreuer–Li relation. Nanotechnol Rev. 2022;11:2061–77.
[57] Shahzad F, Jamshed W, Safdar R, Hussain SM, Nasir NAAM, Dhange M, et al. Thermal analysis characterisation of solar-powered ship using Oldroyd hybrid nanofluids in parabolic trough solar collector: An optimal thermal application. Nanotechnol Rev. 2022;11:2015–37.
[58] Bouslimi J, Alkathiri AA, Alharbi AN, Jamshed W, Eid MR, Bouazizi ML. Dynamics of convective slippery constraints on hybrid radiative Sutterby nanofluid flow by Galerkin finite element simulation. Nanotechnol Rev. 2022;11:1219–36.
[59] Eid MR, Jamshed W, Goud BS, Ibrahim RW, El Din SM, Abd-Elmonem A, et al. Abdalla, Mathematical analysis for energy transfer of micropolar magnetic viscous nanofluid flow on permeable inclined surface and Dufour impact. Case Stud Therm Eng. 2023;49:103211.